see commentary on page 1274

Peroxisome proliferator-activated receptor-α is renoprotective in doxorubicin-induced glomerular injury

Yunfeng Zhou[1,5], Xiaomu Kong[1,5], Pan Zhao[1], Hang Yang[1], Lihong Chen[1], Jing Miao[2], Xiaoyan Zhang[1], Jichun Yang[1], Jie Ding[2] and Youfei Guan[1,3,4]

[1]Department of Physiology and Pathophysiology, Peking University Health Science Center, Beijing, China; [2]Department of Pediatrics, Peking University First Hospital, Beijing, China; [3]Diabetes Center, Peking University Health Science Center, Beijing, China and [4]Key Laboratory of Cardiovascular Science of the Ministry of Education, Peking University Health Science Center, Beijing, China

Doxorubicin (DOX) is an anthracycline antibiotic utilized in antitumor therapy; however, its clinical use is frequently impeded by renal toxic effects. As peroxisome proliferator-activated receptor-α (PPAR-α) has renoprotective effects in drug-related kidney injuries, we tested its ability to inhibit DOX-induced renal injury. Although both male PPAR-α knockout mice and their wild-type littermates (pure 129/SvJ background) had significant proteinuria 4 weeks after DOX treatment, those with deletion of PPAR-α had more severe proteinuria. This was associated with more serious podocyte foot process effacement compared with wild-type mice. In contrast, the PPAR-α agonist fenofibrate effectively reduced proteinuria and attenuated DOX-induced podocyte foot process effacement. Consistently, glomerular nephrin expression was significantly lower in the knockout compared with wild-type mice following DOX treatment. Fenofibrate therapy significantly blunted the reduction in glomerular nephrin levels in DOX-treated wild-type mice. In cultured podocytes, DOX induced apoptosis, increased cleaved caspase-3 levels, and decreased Bcl-2 expression, all attenuated by pretreatment with fenofibrate. Thus, PPAR-α deficiency exacerbates DOX-related renal injury, in part, due to increased podocyte apoptosis.

Kidney International (2011) **79,** 1302–1311; doi:10.1038/ki.2011.17; published online 2 March 2011

KEYWORDS: doxorubicin; fenofibrate; peroxisome proliferator-activated receptor; podocyte injury; proteinuria

Correspondence: *Youfei Guan, Department of Physiology and Pathophysiology, Peking University Health Science Center, 38 Xueyuan Road, Beijing 1000191, China. E-mail: youfeiguan@bjmu.edu.cn*

[5]These authors contributed equally to this work.

Received 15 April 2010; revised 25 November 2010; accepted 21 December 2010; published online 2 March 2011

Doxorubicin (DOX) is an anthracycline antibiotic used widely in antitumor therapy; however, its clinical use can have a cytotoxic effect on several organs, especially the kidney. The toxic effects of doxorubicin on the renal structure are podocyte foot process effacement and increased glomerular permeability, leading to proteinuria.[1–3] The mechanisms involved in DOX-associated nephropathy remain incompletely understood. Among many possible pathogenic factors, oxygen free radicals have been thought to have a critical role.[4,5] Because of this incomplete understanding of underlying mechanisms, the current therapies of DOX-associated nephropathy remain suboptimal, and novel treatments are urgently needed.

Recently, a subfamily of the nuclear receptor transcription factors, peroxisome proliferator-activated receptors (PPARs), including PPAR-α, PPAR-β/δ, and PPAR-γ, has been increasingly recognized as key players in the pathogenesis of metabolic syndrome and its renal complications.[6] PPAR-α, as the first identified PPAR isoform, is a target for various long-chain fatty acids and is predominantly expressed in tissues exhibiting high catabolic rates of fatty acids, such as adipose tissue, liver, heart, muscle, and renal cortex.[7] The actions of PPAR-α are mainly through a ligand-dependent transactivation mechanism, by which PPAR-α heterodimerizes with retinoid X receptor-α and regulates the transcriptional activity of its target genes by binding to the PPAR response element (PPRE) located in the promoter regions of PPAR-α target genes.[8] PPAR-α is highly abundant in the proximal tubules and medullary thick ascending limbs, with lower levels in the glomeruli.[9] In general, PPAR-α controls a set of genes essential for fatty acid β-oxidation and has an important role in the metabolic control of renal energy homeostasis.[10] Besides its role in regulating lipid metabolic role, PPAR-α also shows anti-inflammatory and antifibrotic effects by ligand-dependent transrepressing actions on nuclear factor-κB and activator protein-1 pathways.[11–14] The PPAR-α agonist fenofibrate significantly attenuated but *PPAR-α* gene deficiency markedly worsened albuminuria and glomerular fibrosis in type 2 diabetic db/db mice.[12,13] Recently, activation of PPAR-α by fibrate treatment

was also shown to be effective in ameliorating cisplatin-induced renal tubular injury[15] and DOX-induced apoptosis in renal tubular cells.[16]

Although PPAR-α exerts a renoprotective effect in many renal disorders, whether PPAR-α is involved in the pathogenesis of DOX-associated podocyte injury is unclear. Thus, we aimed to investigate the role of PPAR-α in DOX-induced renal injury *in vivo* and *in vitro* and examine whether PPAR-α activation could represent a preventive maneuver for DOX-associated nephrotoxicity.

RESULTS

Proteinuria and podocyte foot process effacement in DOX-treated wild-type (WT) and PPAR-α knockout mice on a pure 129/SvJ background

Following DOX treatment, both WT and PPAR-$\alpha^{-/-}$ mice on a 129/SvJ background showed significant albuminuria, with more severe proteinuria and hypoalbuminemia in PPAR-$\alpha^{-/-}$ mice than in WT mice (Figure 1). Consistently, DOX-treated PPAR-$\alpha^{-/-}$ mice exhibited higher plasma cholesterol and triglyceride levels than did WT mice (Table 1). Electron microscopy revealed podocyte foot process effacement in both groups (Figure 2A). In each photograph, the mean of the foot process width was calculated as described in the Materials and Methods. As shown in Figure 2B, DOX treatment resulted in more severe podocyte foot process effacement in PPAR-$\alpha^{-/-}$ mice than in WT mice on a 129/SvJ background (foot process width 2446 ± 37.04 vs 854.4 ± 30.94 nm, $P<0.01$).

Glomerular expression of nephrin in DOX-treated WT and PPAR-$\alpha^{-/-}$ mice on a pure 129/SvJ background

The expression of nephrin in the glomeruli and the kidneys was measured by immunohistochemistry and real-time PCR (RT-PCR), respectively. As expected, strong glomerular nephrin immunoreactivity was observed in WT mice (Figure 3A). Although the expression of nephrin was markedly decreased in the glomeruli of both DOX-treated WT and PPAR-$\alpha^{-/-}$ mice, nephrin immunoreactivity was significantly lower in PPAR-$\alpha^{-/-}$ than in WT mice after DOX treatment (Figure 3A and B). RT-PCR analysis of renal nephrin expression further showed that the levels of nephrin mRNA expression was significantly lower in PPAR-$\alpha^{-/-}$ than in WT mice after DOX treatment (Figure 3C).

Effect of PPAR-α agonist fenofibrate on proteinuria and podocyte foot process effacement in DOX-treated WT mice on both 129/SvJ and BALB/c backgrounds

Treatment with a PPAR-α agonist fenofibrate for 1 month significantly reduced the level of DOX-induced proteinuria, although the levels remained higher than that in controls (Figure 4a). DOX-treated mice exhibited decreased plasma albumin levels, with no significant difference in levels between DOX and fenofibrate-treated mice (Figure 4b). Plasma cholesterol and triglyceride levels showed a slight but not significant increase in the DOX group (Table 2). Electron microscopy revealed DOX-treated mice with more severe podocyte foot process effacement than control mice, and fenofibrate treatment significantly improved podocyte foot process effacement induced by DOX (Figure 5).

We further verified the renoprotective role of PPAR-α in DOX-induced renal injury in mice of a pure BALB/c background. Consistent with the findings observed in 129/SvJ mice, PPAR-α agonist fenofibrate significantly improved DOX-associated nephropathy in BALB/c mice (Supplementary Figures S1–4 online). Fenofibrate treatment significantly reduced proteinuria levels and attenuated podocyte foot

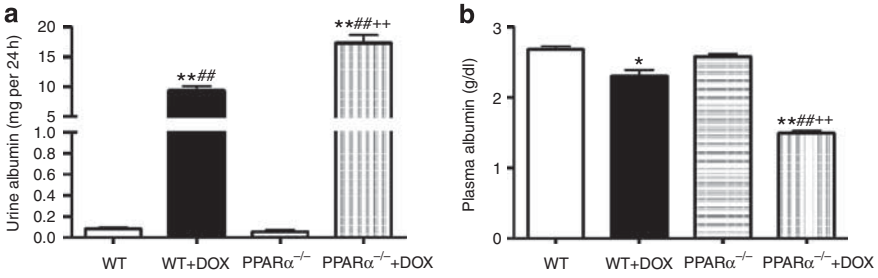

Figure 1 | Changes in proteinuria (a) and plasma albumin (b) levels in doxorubicin (DOX)-treated wild-type (WT) and peroxisome proliferator-activated receptor-α (PPAR-α) knockout mice. Data are means ± s.e.m. $^{*}P<0.05$, $^{**}P<0.01$ vs WT; $^{\#\#}P<0.01$ vs PPAR-$\alpha^{-/-}$; $^{++}P<0.01$ vs WT + DOX, $N=5$.

Table 1 | Metabolic and physiological parameters in DOX-treated WT and PPAR-α knockout mice

	WT	WT+DOX	PPAR-$\alpha^{-/-}$	PPAR-$\alpha^{-/-}$+DOX
Body weight (g)	26.76 ± 0.55	25.22 ± 0.51	25.12 ± 0.41	20.74 ± 0.83$^{**,\#\#,++}$
Liver/body weight (%)	3.99 ± 0.10	4.32 ± 0.11	4.21 ± 0.11	5.50 ± 0.16$^{**,\#\#,++}$
Kidney/body weight (%)	0.69 ± 0.01	0.65 ± 0.02	0.65 ± 0.03	0.60 ± 0.02
Fat/body weight (%)	1.61 ± 0.19	1.50 ± 0.27	1.83 ± 0.14	0.69 ± 0.04$^{**,\#\#,++}$
Plasma cholesterol (mg/dl)	114.8 ± 11.18	198.4 ± 36.01	136.6 ± 15.27	390.2 ± 23.89$^{**,\#\#,++}$
Plasma triglyceride (mg/dl)	98.72 ± 10.98	173.3 ± 28.04	112.9 ± 12.24	296.8 ± 30.57$^{**,\#\#,++}$

Abbreviations: DOX, doxorubicin; PPAR-α, peroxisome proliferator-activated receptor-α; WT, wild type.
$^{*}P<0.01$ vs WT; $^{\#\#}P<0.01$ vs PPAR-$\alpha^{-/-}$; $^{++}P<0.01$ vs WT+DOX.

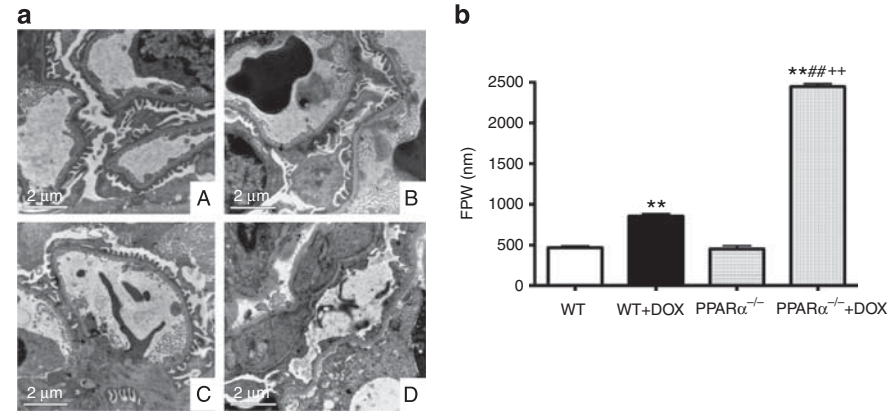

Figure 2 | Doxorubicin (DOX)-induced podocyte foot process effacement in peroxisome proliferator-activated receptor-α (PPAR-α) wild-type (WT) and knockout mice. (**a**) Representative electron microscopy images of podocyte foot processes: (A) WT; (B) WT with DOX (WT + DOX); (C) PPAR-α knockout (PPAR-$\alpha^{-/-}$); (D) PPAR-α knockout with DOX (PPAR-$\alpha^{-/-}$ + DOX). (**b**) Quantification of foot process effacement. Data are means ± s.e.m. $^{**}P<0.01$ vs WT; $^{\#\#}P<0.01$ vs PPAR-$\alpha^{-/-}$; $^{++}P<0.01$ vs WT + DOX, $N=5$.

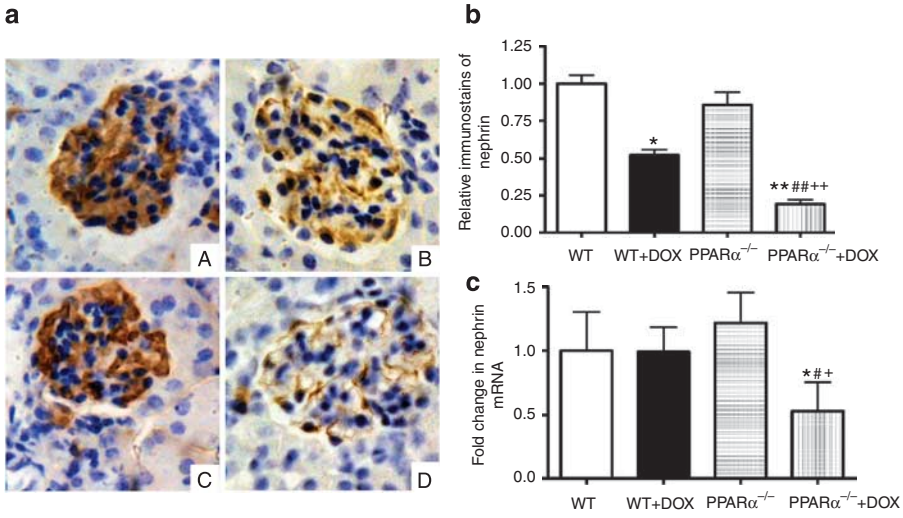

Figure 3 | Immunohistochemistry and quantitative real-time PCR analysis of nephrin expression in the glomeruli of wild-type (WT) and peroxisome proliferator-activated receptor-α (PPAR-α) knockout mice receiving doxorubicin (DOX) treatment. Downregulated expression of nephrin was observed in both DOX-treated WT and PPAR-α knockout mice. (**a**) Representative immunohistochemical stainings for nephrin: (A) WT; (B) WT with DOX (WT + DOX); (C) PPAR-α knockout (PPAR-$\alpha^{-/-}$); and (D) PPAR-α knockout with DOX (PPAR-$\alpha^{-/-}$ + DOX). (**b**) Semiquantification of nephrin protein immunoreactivity in each group. (**c**) Real-time PCR assay confirmed downregulated expression of nephrin in DOX-treated PPAR-α knockout mice. Data are means ± s.e.m. $^{*}P<0.05$, $^{**}P<0.01$ vs WT; $^{\#}P<0.05$, $^{\#\#}P<0.01$ vs PPAR-$\alpha^{-/-}$; $^{+}P<0.05$, $^{++}P<0.01$ vs WT + DOX, $N=5$.

process effacement (Supplementary Figure S1 online). Fenofibrate treatment also lowered blood urea nitrogen levels and reduced urinary KIM-1 (kidney injury molecule-1) excretion (Supplementary Figure S2 online). Glomeruloscelerosis and tubulointerstitial fibrosis were markedly ameliorated after fenofibrate treatment (Supplementary Figure S3 online). Moreover, fenofibrate treatment significantly restored glomerular nephrin expression in DOX-treated BALB/c mice (Supplementary Figure S4 online). Collectively, these results confirm the findings in 129/SvJ mice and support our conclusion that PPAR-α agonists represent potential preventive agents for DOX-induced nephropathy.

Effect of fenofibrate on proteinuria and podocyte foot process effacement in DOX-treated *PPAR-α* gene knockout mice

We examined the protective effect of fenofibrate on DOX-induced renal injury in *PPAR-α* gene knockout mice (Supplementary Figures S5–8 online). The results showed that fenofibrate had little effect on proteinuria (Supplementary Figure S5A online), plasma albumin levels (Supplementary Figure S5B online), podocyte foot process effacement (Supplementary Figure S5C and D online), blood urea nitrogen and serum creatinine levels (Supplementary Figure S6A and B online), urinary KIM-1 excretion (Supplementary Figure S6C online), glomerular histology (Supplementary

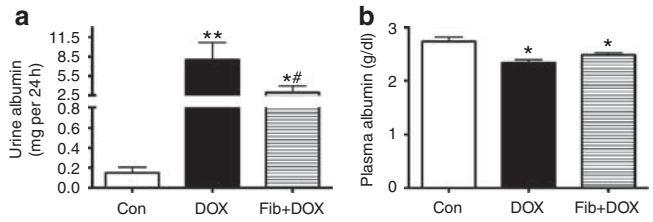

Figure 4 | The effect of fenofibrate treatment on (a) proteinuria and (b) plasma albumin levels in doxorubicin (DOX)-treated mice. Data are means ± s.e.m. $^{*}P<0.05$, $^{**}P<0.01$ vs control (Con); $^{\#}P<0.05$ vs DOX, $N=5$.

Figure S7 online), and nephrin expression (Supplementary Figure S8 online) in PPAR-α knockout mice.

Effect of fenofibrate treatment on glomerular expression of nephrin in mice receiving DOX treatment

The immunoreactivity of nephrin was markedly decreased in glomeruli from DOX-treated mice on a pure 129/SvJ background, which was significantly improved by fenofibrate treatment by immunohistochemistry (Figure 6A and B). RT-PCR analysis further revealed that fenofibrate treatment increased nephrin mRNA expression in DOX-treated mice (Figure 6D). Immunofluorescence study demonstrated that nephrin distribution was changed from a fine, linear-like to discontinuous, coarse granular pattern in control mouse after DOX treatment, which was attenuated by treatment with fenofibrate (Figure 6C).These findings further support the results of electron microscopy studies on podocytes shown in Figures 2 and 5. Similarly, fenofibrate treatment also significantly improved the DOX-induced decrease in nephrin expression at both mRNA and protein levels in BALB/c mice (Supplementary Figure S4 online).

PPAR-α expression in kidney, renal glomeruli, and cultured podocytes

Although PPAR-α is abundantly expressed in the proximal tubules and medullary thick ascending limbs, as assessed by *in situ* hybridization[9] and immunohistochemistry (Supplementary Figure S9A online), low but functional PPAR-α expression was also reported in glomerular cells including mesangial cells and podocytes.[6,8] Using RT-PCR, we found that PPAR-α was constitutively expressed in freshly isolated mouse glomeruli (Supplementary Figure S9B online). RT-PCR, western blot analysis, and PPRE 3× luciferase reporter analysis further revealed the presence of PPAR-α in podocytes. Both PPAR-α mRNA and protein were detected in culture podocytes (Figure 7a). PPRE luciferase reporter analysis further demonstrated that fenofibrate treatment significantly increased luciferase activity in podocytes (Figure 7b), which suggests a functional expression of PPAR-α in these cells. To test whether DOX suppression of PPRE-Luc activity is specific to the PPAR-α pathway, we cultured primary glomerular mesengial cells from PPAR-α knockout mice. As shown in Supplementary Figure S10 online, DOX significantly reduced PPRE-luciferase activity as seen in podocytes, and fenofibrate treatment did not increase PPRE activity in PPAR-α-deficient mesengial cells. It implies that DOX-suppressed PPRE-luciferase activity may be shared among signaling cascades downstream PPAR-β and/or PPAR-γ.

Table 2 | Metabolic and physiological parameters in DOX-treated mice with or without fenofibrate treatment

	Con	DOX	Fib+DOX
Body weight (g)	25.95 ± 1.05	24.35 ± 0.33	23.78 ± 0.49
Liver/body weight (%)	3.93 ± 0.24	4.21 ± 0.37	5.37 ± 0.45$^{*,\#}$
Kidney/body weight (%)	0.69 ± 0.03	0.67 ± 0.03	0.66 ± 0.02
Fat/body weight (%)	1.41 ± 0.10	1.24 ± 0.12	0.86 ± 0.11$^{*,\#}$
Plasma cholesterol (mg/dl)	96.98 ± 7.56	138.2 ± 16.73	86.99 ± 11.36
Plasma triglyceride (mg/dl)	83.94 ± 12.49	116.3 ± 21.74	80.42 ± 12.95

Abbreviations: Con, control; DOX, doxorubicin; Fib, fenofibrate.
$^{*}P<0.05$ vs Con; $^{\#}P<0.05$ vs DOX.

Decreased PPAR-α expression in DOX-treated mouse kidneys and cultured podocytes

Renal PPAR-α expression and localization was further analyzed using RT-PCR and immunohistochemistry. DOX treatment resulted in a significant reduction in PPAR-α mRNA and protein levels in whole kidneys (Supplementary Figure S9A and C online), with little effect on intrarenal localization of PPAR-α protein (Supplementary Figure S9A online). Consistently, DOX-treated podocytes exhibited reduced PPAR-α mRNA levels (Supplementary Figure S9D online) and endogenous PPAR-α activity (Figure 7b). As expected, PPAR-α expression was not present in *PPAR-α* gene-deficient mice (Supplementary Figure S9E online), and its level in podocytes was lower than in the glomeruli and the kidneys (Supplementary Figure S9F online). Interestingly, PPAR-α activation by fenofibrate treatment attenuated the inhibitory effect of DOX on PPAR-α transcription activity (Figure 7b). Fenofibrate treatment also increased transcription of PPAR-α target genes *CYP4A10* and *CYP4A14*, although DOX-treated podocytes only slightly decreased the expression of these genes (Figure 7c and d).

Fenofibrate treatment protected podocytes against DOX-induced apoptosis

Fluorescence-activated cell sorting was performed to measure apoptosis. Podocytes were stained with Annexin V–fluorescein isothiocyanate and propidium iodide to distinguish viable, apoptotic, and necrotic cells. As expected, DOX induced significant apoptosis compared with untreated cells and fenofibrate treatment significantly attenuated DOX-induced apoptosis. Fenofibrate alone did not affect apoptosis in normal podocytes (Figure 8a). These findings were further supported by a significant reduction in DOX-induced glomerular cell apoptosis after fenofibrate treatment (Supplementary Figure S11 online).

In line with these apoptotic changes, Bcl-2 (B-cell lymphoma 2) mRNA expression was significantly decreased and Bax mRNA expression increased in response to DOX treatment. However, pretreatment with fenofibrate restored Bcl-2 and Bax expression to control levels (Figure 8b). Consistently, protein expression of a key downstream effector of apoptosis, cleaved caspase-3, was significantly increased after DOX injury, whereas preincubation with fenofibrate significantly ameliorated the increased caspase-3

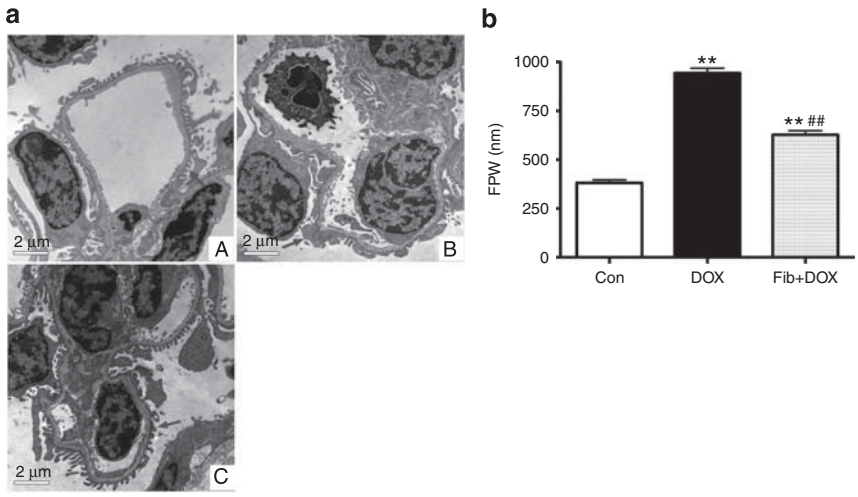

Figure 5 | Fenofibrate treatment ameliorated podocyte foot process effacement in doxorubicin (DOX)-treated mice. (**a**) Representative electron microscope images of podocyte foot processes: (A) control (Con); (B) DOX (DOX); and (C) fenofibrate + DOX (Fib + DOX). (**b**) Quantification of foot process effacement. Data are means ± s.e.m. $^{**}P<0.01$ vs Con; $^{\#\#}P<0.01$ vs DOX, $N=5$.

activity (Figure 8c). It was also noticed that DOX treatment resulted in a significant increase in reactive oxygen species production, which was attenuated by treatment with fenofibrate (Supplementary Figure S12 online).

Time course difference of DOX-associated nephropathy between 129/SvJ and BALB/c mice

To determine whether mice on a 129/SvJ genetic background behave similarly to BALB/c mice during the DOX experiment, we performed a study characterizing the course of DOX nephrotoxicity in both 129/SvJ and BALB/c strains. As shown in Supplementary Figures S13–16 online, a 6-week treatment of DOX continuously increased proteinuria levels (Supplementary Figure S13A online) and decreased plasma albumin concentrations (Supplementary Figure S13B online) in 129/SvJ mice. Starting from week 4, podocyte foot process effacement appeared and became more severe at week 6 (Supplementary Figure S13C and D online). Blood urea nitrogen and urinary KIM-1 excretion were significantly increased after 4 weeks of DOX treatment and became much higher after 6 weeks of DOX exposure (Supplementary Figure S14 online). Furthermore, podocyte nephrin expression was much lower in the 6-week DOX-treated mice than in the 4-week DOX-treated mice (Supplementary Figure S16 online). Compared with BALB/c mice, in which glomerular sclerosis and tubulointerstitial fibrosis became evident at week 4 (Supplementary Figure S3 online), 129/SvJ mice only exhibited such changes 6 weeks after DOX treatment (Supplementary Figure S15 online).

DISCUSSION

Increasing evidence suggests that PPAR-α may exert renoprotective effect in the kidney.[17–19] This study examined the role of PPAR-α in DOX-induced podocyte injury *in vivo* and *in vitro*. PPAR-$\alpha^{-/-}$ mice showed more severe urine protein excretion and podocyte foot process effacement than WT mice after DOX treatment. In contrast, fenofibrate treatment effectively reduced proteinuria and ameliorated podocyte foot process effacement in DOX-treated mice. In cultured podocytes, fenofibrate protected against DOX-induced apoptosis. These observations suggest that PPAR-α may participate in the pathogenesis of DOX-induced glomerular podocyte injury and represent a promising preventive target for DOX-associated glomerulopathy.

Although PPAR-α activation exerts a beneficial renal effect in DOX-associated renal injury, the underlying mechanisms of how PPAR-α agonist protects against DOX-induced kidney damage remain elusive. A study of diabetic nephropathy showed that fenofibrate markedly attenuated albuminuria and renal fibrosis in a murine model of type 2 diabetes (db/db mice).[13] In contrast, *PPAR-α* gene deficiency was found to be associated with exacerbated diabetic nephropathy, with more severe albuminuria and worsened renal injury.[12] In several tubular injury models, PPAR-α activation prevented cisplatin-induced renal tubular injury[15] and protected renal tubular cells against DOX-induced apoptosis[16] and acute fatty acid toxicity.[20] Our findings that PPAR-α protects DOX-induced podocyte damage extend previous observations of the fibrate class of PPAR-α agonists conferring a renoprotective effect in type 2 diabetes[21–23] and cisplatin-induced nephropathy.[15,24]

In the present studies, we found that DOX treatment significantly decreased PPAR-α expression in the kidneys and cultured podocytes, suggesting that DOX-induced renal injury may be associated with decreased PPAR-α activity. In support of this, glomerular expression of nephrin was much lower in PPAR-$\alpha^{-/-}$ mice than WT mice after DOX treatment. After DOX treatment, the normal, fine linear staining pattern of nephrin almost completely disappeared and a discontinuous, coarse granular pattern was observed. These observations suggest that *PPAR-α* gene deficiency was associated with exacerbated DOX-associated podocyte

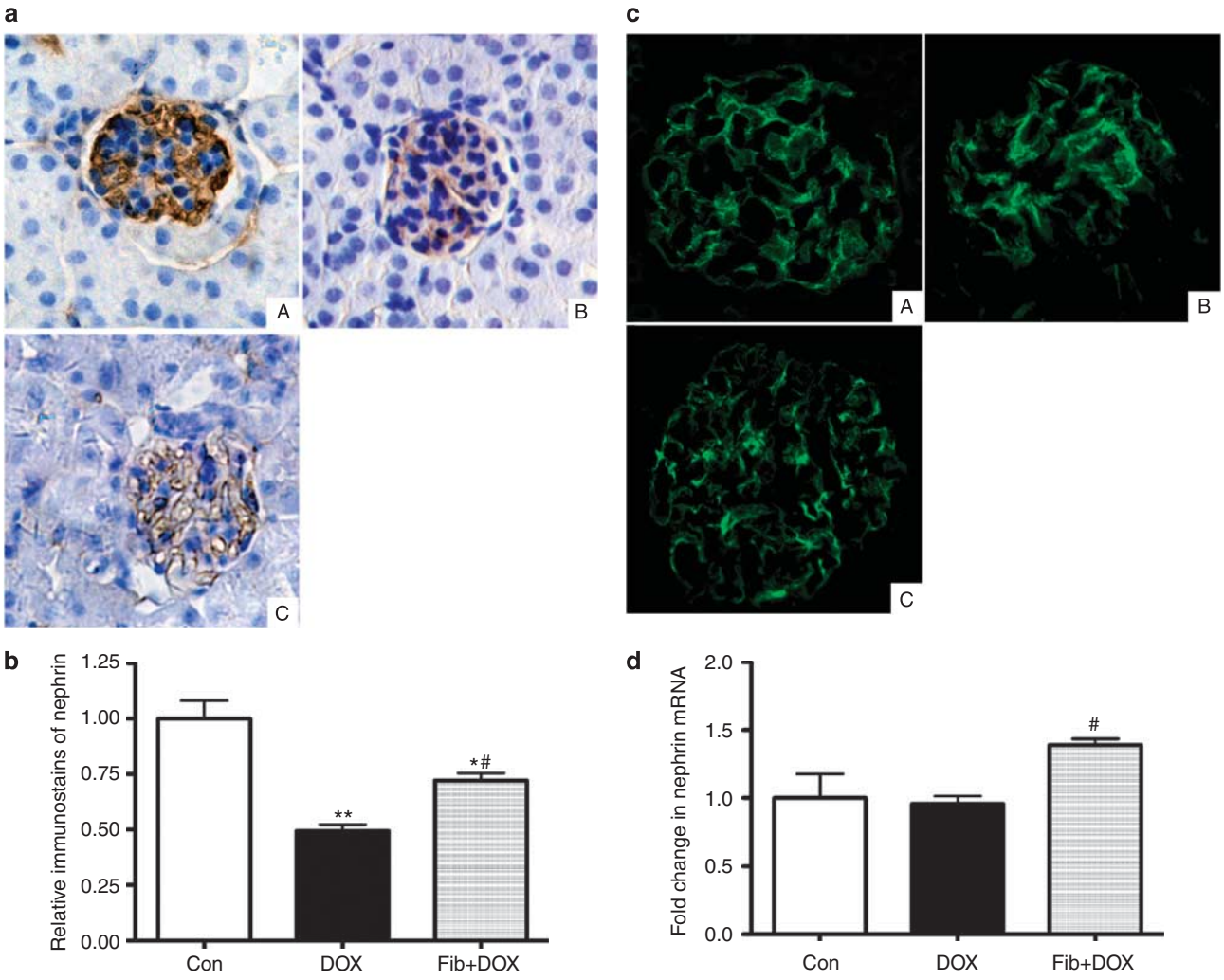

Figure 6 | Immunohistochemistry, immunofluorescence, and quantitative real-time PCR analysis of nephrin expression in the glomeruli of doxorubicin (DOX)-treated mice in the presence or absence of fenofibrate treatment. (**a**) Representative immunostainings for nephrin by immunohistochemistry: (A) control (Con); (B) DOX (DOX); and (C) fenofibrate + DOX (Fib + DOX). (**b**) Semiquantification of nephrin protein immunoreactivity in each group. (**c**) Representative immunostainings for nephrin by immunofluorescence: (A) in control mice, nephrin staining was detected as a fine, linear-like pattern along the glomerular capillary loop, whereas in DOX-treated mice (B) the linear staining of nephrin disappeared completely, and a discontinuous, coarse granular pattern was observed. After fenofibrate treatment (C) the changes were less serious than those in DOX-treated mice, and linear pattern of staining of nephrin could be detected in most parts of the glomerular capillary wall. (**d**) Real-time PCR assay demonstrated that fenofibrate treatment increased nephrin mRNA expression in DOX-treated mice. Data are means ± s.e.m. $^{*}P<0.05$, $^{**}P<0.01$ vs Con; $^{\#}P<0.05$ vs DOX, $N=5$.

damage and PPAR-α activation may be renoprotective in DOX-treated mice. In fact, after treatment with fenofibrate, DOX-induced downregulation and changes in expression pattern of nephrin was significantly restored. These findings are generally in agreement with a previous report in which PPAR-α activation in podocytes caused an increased nephrin expression by stimulating nephrin promoter activity and reducing nephrin mRNA degradation.[25] Therefore, it is reasonable to postulate that PPAR-α agonist exerts a renoprotective effect in DOX-induced renal injury, at least in part, by increasing nephrin expression and maintaining the integrity of podocytes.

A large amount of evidence suggests that genetic background has a strong influence on disease course and severity. This study demonstrates that DOX can induce glomerular sclerosis and tubulointerstitial fibrosis in both 129/SvJ and BALB/c mice, with the latter being more susceptible.[26,27] Although in 129/SvJ mice, tubulointerstitial fibrosis did not occur until 6 weeks after DOX treatment, dysfunction of renal tubules was evident at week 4. These observations suggest that although it requires longer treatment for DOX to induce glomerular sclerosis and tubulointerstitial fibrosis in 129/SvJ mice, they behave similarly to BALB/c mice after DOX treatment. More importantly, PPAR-α agonist fenofibrate was effective in attenuating DOX-induced renal injury in both 129/SvJ and BALB/c mice.

The podocyte is believed to be the site of the initial injury in proteinuric renal diseases, including DOX-related

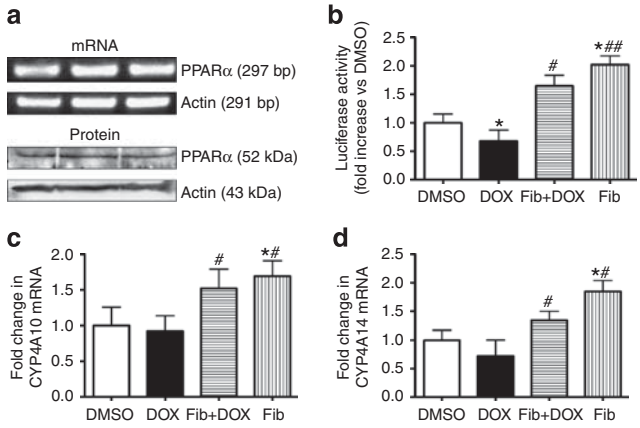

Figure 7 | Peroxisome proliferator-activated receptor-α (PPAR-α) expression and transcriptional activity in podocytes. (**a**) Detection of PPAR-α mRNA and protein expression in culture podocytes. (**b**) Ligand-induced transcriptional activity of PPAR-α. Note that doxorubicin (DOX) reduced PPAR response element (PPRE)-luciferase activity and fenofibrate treatment significantly increased PPAR-α transcriptional activity in podocytes. (**c**) Real-time PCR assay demonstrated that fenofibrate treatment increased CYP4A10 mRNA expression in DOX-treated podocytes. (**d**) Real-time PCR assay demonstrated that fenofibrate treatment increased CYP4A14 mRNA expression in DOX-treated podocytes. Data are means ± s.e.m. $^{*}P<0.05$ vs dimethylsulfoxide (DMSO); $^{\#}P<0.05$, $^{\#\#}P<0.01$ vs DOX, $N=3$.

nephropathy. In this study, we found PPAR-α was constitutively expressed in renal glomeruli and was functional in cultured podocytes, and DOX treatment significantly reduced its expression. The PPAR-α agonist fenofibrate protected podocytes against DOX-induced apoptosis. This is consistent with the finding that fenofibrate treatment significantly reduced apoptotic cell numbers in the glomeruli of mice treated with DOX. Therefore, the direct actions on podocytes may represent a major mechanism involved in the renoprotective effect of fenofibrate in DOX-associated podocyte injury.

Our finding of the PPAR-α agonist fenofibrate markedly reducing DOX-induced apoptosis in cultured podocytes was associated with increased antiapoptotic Bcl-2 expression, decreased proapoptotic Bax expression, and reduced cleaved caspase-3 levels. These findings suggest that PPAR-α may act as an important protective factor in podocytes, and the fibrate class of PPAR-α agonists may ameliorate DOX-induced podocyte death and detachment via blocking the apoptotic signal.

In the present studies, we demonstrated that activation of PPAR-α confers protective effects in DOX-induced podocyte injury *in vitro* and attenuates proteinuria, podocyte foot effacement, and tubulointerstitial fibrosis *in vivo*. Fenofibrate

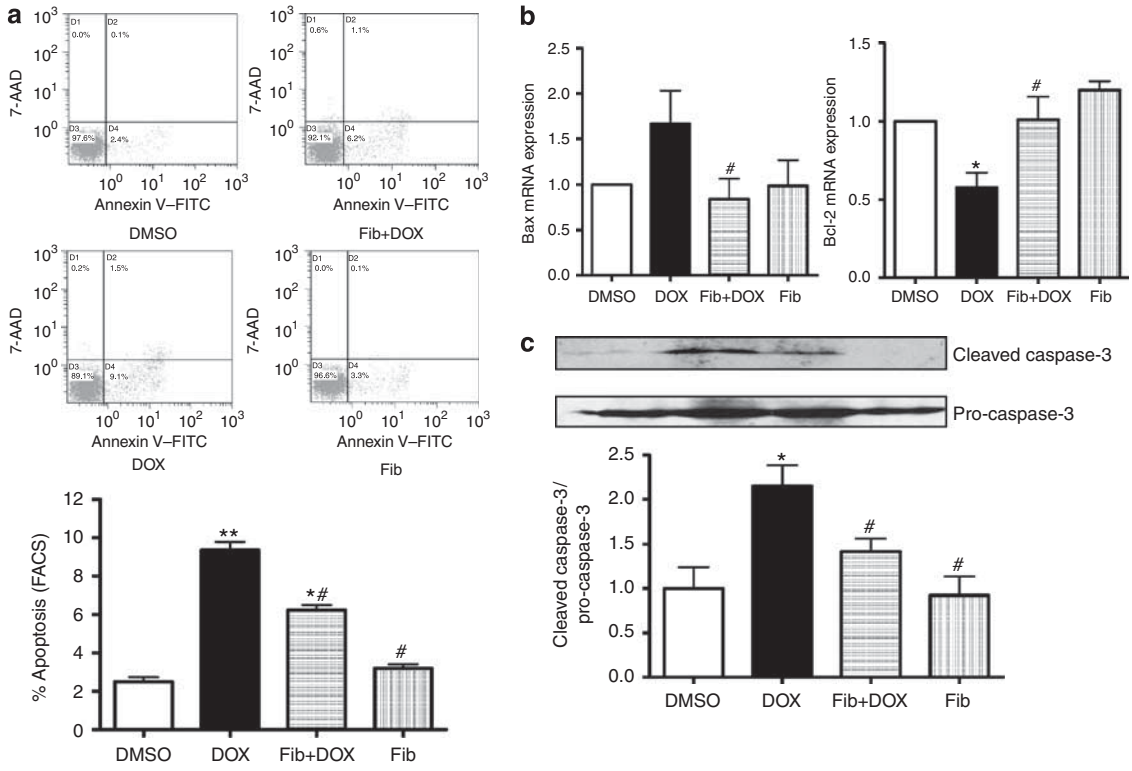

Figure 8 | Fenofibrate treatment protected podocytes against doxorubicin (DOX)-induced apoptosis. (**a**) Fluorescence-activated cell sorting (FACS) analysis of apoptotic cells. DOX treatment significantly induced podocyte apoptosis, which was markedly attenuated by fenofibrate treatment. $^{*}P<0.05$, $^{**}P<0.01$ vs dimethylsulfoxide (DMSO); $^{\#}P<0.05$ vs DOX, $N=3$. (**b**) mRNA expression of proapoptotic Bax and antiapoptotic B-cell lymphoma 2 (Bcl-2) in podocytes. $^{*}P<0.05$ vs DMSO; $^{\#}P<0.05$ vs DOX, $N=3$. (**c**) Activated caspase-3 expression in podocytes with DOX and effect of fenofibrate on the expression. Data are means ± s.e.m. $^{*}P<0.05$ vs DMSO; $^{\#}P<0.05$ vs DOX, $N=3$.

treatment also shows a protective effect on tubular function as reflected by a marked reduction in urinary KIM-1 excretion. However, we cannot rule out the possibility that the role of PPARα in other glomerular cells and tubular cells also contributes to beneficial effects of fenofibrate in DOX-associated nephropathy, as it has been previously reported that PPAR-α was functionally expressed in glomerular mesangial cells, endothelial cells, and proximal tubule cells.[6,8] The beneficial effect of fenofibrate on these cells may also contribute to the renoprotective effect in DOX-treated mice.

Hyperlipidemia is one of the major features in DOX-induced nephropathy.[28,29] Our previous study demonstrated that hyperlipidemia is associated with increased transcription activity of SREBP-1 (sterol regulatory element binding protein-1) and enhanced lipogenesis in the liver.[30] Increasing evidence suggests that hyperlipidemia and renal lipotoxicity are important pathogenic factors in kidney damage,[31,32] and may contribute to the development and the progression of DOX-associated nephropathy.

In summary, *PPAR-α* gene deficiency was associated with exacerbated DOX nephropathy, with worsened proteinuria due to podocyte injury. The PPAR-α agonist fenofibrate was effective in ameliorating podocyte injury via maintaining podocyte viability and integrity. The PPAR-α agonist fenofibrate may represent a promising preventive agent in treating DOX nephropathy.

MATERIALS AND METHODS

Animal treatment

Male PPAR-α knockout (PPAR-$\alpha^{-/-}$) mice and sex- and age-matched WT littermates (8–10 weeks old, 22–28 g) on a pure 129/SvJ background (Jackson Lab, Bar Harbor, ME) were used and approved by the animal experimentation committee of Peking University Health Science Center. To test the effect of *PPAR-α* gene deficiency on DOX (doxorubicin hydrochloride; Sigma, St Louis, MO)-induced renal damage, mice were divided into four groups of animals for treatment: (1) WT; (2) WT mice treated with DOX (WT + DOX); (3) PPAR-α knockout mice (PPAR-$\alpha^{-/-}$); and (4) PPAR-α knockout mice treated with DOX (PPAR-$\alpha^{-/-}$ + DOX). DOX was injected intravenously twice on days 1 and 14 (10 mg/kg). An equivalent volume of saline was injected into control groups. To test whether PPAR-α activation attenuates DOX-associated kidney injury, WT animals were assigned to three groups for treatment: (1) control mice (Con); (2) mice treated with DOX (DOX); and (3) DOX-treated mice fed a chow diet supplemented with 0.2% fenofibrate (w/diet w; Sigma) for 7 days before DOX injection (Fib + DOX).[13] To measure 24-h proteinuria, mice were placed in individual mouse metabolic cages (Tecniplast, Buguggiate, Italy) with free access to water and food. At week 4, mice were killed, and their kidneys were removed for examination by light and electron microscopy and immunohistochemical and immunofluorescence study.

Biochemical measurement of blood and urine samples

Plasma concentrations of total cholesterol, triglycerides, and albumin were measured using an autoanalyzer (Hitachi 7170A, Tokyo, Japan). Urinary albumin excretion was assayed with a mouse albumin enzyme-linked immunosorbent assay quantitation kit (Bethyl, Montgomery, TX).

Electron microscopy and measurement of podocyte foot process effacement

For electron microscopy examination, renal cortex samples were minced into 1-mm^3 pieces on ice, immediately fixed in 2.5% buffered glutaraldehyde, and embedded in epoxy resin. Ultrathin sections (0.1 μm thick) were examined by electron microscopy. To study slit diaphragm morphology, random photographs were taken at a final magnification of ×10,000. Three glomeruli per mouse were evaluated on five 10K images/glomerulus. Electron microscopy images were analyzed using ImageJ (NIH Image, Bethesda, MD), and the method of measuring podocyte foot process effacement was adapted from a previous report.[33] From each photograph, the mean of the foot process width was calculated as follows: foot process width = $\pi/4 \times (\sum$GBM length/$\sum$foot process).

Immunohistochemistry studies

Kidneys were fixed in 4% paraformaldehyde overnight at 4 °C. After blocking for 20 min with blocking solution (1% bovine serum albumin), the sections at 4 μm were incubated with primary antibodies against nephrin (N-20; Santa Cruz, CA) and PPAR-α (H-98; Santa Cruz) overnight at 4 °C, respectively. Sections were examined in a masked manner on light microscopy (Olympus BX-50; Olympus Optical, Tokyo, Japan). For quantification of the proportional area of staining, 20 views (×400 magnification) were randomly located in the glomerulus of each slide (Scion Image Beta 4.0.2; Scion, Frederick, MD).

Indirect immunofluorescence studies

The indirect immunofluorescence was performed to examine nephrin expression in the glomeruli. The slides were fixed in ice-cold acetone for 10 min, subsequently permeabilized with 0.5% Triton X-100 for 15 min, and then blocked with blocking solution (1% bovine serum albumin) for 30 min. The slides were incubated overnight with rabbit polyclonal anti-mouse nephrin antibody (kindly supplied by Professor Karl Tryggvason, Sweden) at 4 °C and then incubated with the fluorescein isothiocyanate-conjugated anti-rabbit IgG antibody. Images were obtained by confocal laser-scanning microscopy using a Bio-Rad Radiance 2100 TM confocal system (Philadelphia, PA) attached to a Nikon TE 300 microscope (Tokyo, Japan). A total of 20 glomeruli views per slide were randomly obtained with a digital camera at ×400 magnification.

Cell culture and treatment

Studies involved use of a conditionally immortalized mouse podocyte cell line as described previously.[34] Podocytes were cultured in RPMI-1640 media (Gibco, Gaithersburg, MD) containing 10% fetal bovine serum (Hyclone, Logan, UT), 100 U/ml penicillin, and 100 μg/ml streptomycin. Podocytes were propagated in a medium containing 10 U/ml mouse interferon-γ (R&D Systems, Minneapolis, MN) at 33 °C. To initiate differentiation, cells were plated in collagen type I-coated flasks under the nonpermissive condition (37 °C without interferon-γ) for 7–10 days. Podocyte injury was induced by treatment with 0.5 μmol/l DOX for 24 h. To determine the role of PPAR-α in DOX-induced podocyte injury, fully differentiated podocytes were preincubated for 6 h with a PPAR-α agonist, fenofibrate (10 μmol/l), before DOX exposure. All cellular experiments were performed a minimum of three times, unless otherwise indicated.

Analysis of endogenous PPAR-α transcription activity in cultured podocytes

PPAR-α transcriptional activity was measured as previously described[35] using the pTK-(ACO3)-Luc reporter construct containing three

copies of the acetyl-CoA oxidase promoter PPRE. Podocytes grown in six-well plates were transiently transfected with 5 μg of reporter construct and 0.5 μg β-galactosidase plasmid as an internal control using the VigoFect reagent (Vigorous, Beijing, China) for 48 h. Cells were then incubated with fenofibrate or vehicle for 6 h, before DOX exposure. Luciferase activity was measured using a luciferase assay system (Promega, Madison, WI). Transfection efficiency was normalized to β-galactosidase activity and expressed as fold induction of vehicle-treated control cells. Transfection of plasmids did not result in cytotoxicity of podocytes (Supplementary Figure S17 online).

Detection of apoptosis

The percentage of podocyte apoptosis was measured and quantitated by fluorescence-activated cell sorting. Briefly, cells were grown to 90% confluency on culture dishes, and treated with fenofibrate with or without DOX as described above. Cells were then washed twice with ice-cold phosphate-buffered saline, trypsinized, and pelleted by centrifugation at 200 g for 5 min. The pellets were washed once with phosphate-buffered saline, transferred to 5 ml culture tubes, and resuspended in 2 μl of propidium iodide dye and 2 μl of Annexin V-fluorescein isothiocyanate (Roche, Indianapolis, IN). To each tube, 400 μl binding buffer was added. The cells were then analyzed for apoptosis using FACScalibur (BD Biosciences, San Jose, CA). Cells positive for Annexin V–fluorescein isothiocyanate and negative for propidium iodide were deemed apoptotic.

Quantitative RT-PCR

Total RNA was extracted from kidneys and podocytes. For each RNA sample, 2 μg was reverse-transcribed and resultant cDNA samples were then used as templates for quantitative PCR. RT-PCR analysis involved use of SYBR Green (Invitrogen, Carlsbad, CA) according to the manufacturer's instructions. Primers designed to target mouse PPAR-α, nephrin, Bax, Bcl-2, CYP4A10, and CYP4A14 were as follows: PPAR-α, 5′-CGTTCCAGCCCTTCCTCAGTCAGC-3′ (sense), 5′-GACATCCCGACAGACAGGCACTTG-3′ (antisense); nephrin, 5′-CCCAACACTGGAAGAGGTGT-3′ (sense), 5′-CTGGTCGTAGATT CCCCTTG-3′ (antisense); Bax, 5′-TGCAGAGGATGATTGCTGAC-3′ (sense), 5′-GATCAGCTCGGGCACTTTAG-3′ (antisense); Bcl-2, 5′-AGGAGCAGGTGCCTACAAGA-3′ (sense), 5′-GCATTTTCCCAC CACTGTCT-3′ (antisense); CYP4A10, 5′-GACAAGGACCTACG TGCTGAGG-3′ (sense), 5′-CTCATAGCAAATTGTTTCCCA-3′ (antisense); CYP4A14, 5′-CCCACAGGGACATGCAGATTAG-3′ (sense), 5′-CACACAGAGCTCGGAAGACC-3′ (antisense). The PCR reactions were carried out at 94 °C for 5 min, followed by 35 cycles of 94 °C for 30 s, 58–62 °C for 30 s and 72 °C for 30 s, with a final extension at 72 °C for 5 min. Actin was used as an internal control.

Western blot analysis of caspase-3

An amount of 40 μg protein samples was transferred to nitrocellulose membrane (Applygen, Beijing, China). The membrane was washed and blocked in 1 × phosphate-buffered saline with 0.02% Tween-20 supplemented with 5% skim milk powder for 1 h at room temperature with gentle shaking, and then incubated overnight (4 °C) with the following primary antibodies: anti-cleaved caspase-3 antibody (Asp 175, Cat no. 9661; Cell Signaling Technology, Boston, MA) or anti-pro-caspase-3 antibody (Cat no. 9662; Cell Signaling Technology). The membrane was washed three times for 30 min in 1 × phosphate-buffered saline with 0.02% Tween-20 and then incubated with horseradish peroxidase-conjugated secondary antibodies for 1 h at room temperature. After being washed three times, the membrane was then transferred to the ECL Reagent (Applygen) and exposed to XBT-1 film (Kodak, Rochester, NY).

Statistical analysis

Data are shown as means ± s.e.m. using GraphPad Prism software (GraphPad Software, La Jolla, CA). Analysis involved analysis of variance and Student's *t*-test. A $P<0.05$ was considered statistically significant.

DISCLOSURE

All the authors declared no competing interests.

ACKNOWLEDGMENTS

This work was supported by the National Natural Science Foundation of China (NSFC) grants 30890041/81030003/30870905/30725033, the Ministry of Science and Technology (2010CB912503), and the National Institute of Diabetes and Digestive and Kidney Diseases (NIDDK RO1 065074-04 & PPG 038226 to YG).

SUPPLEMENTARY MATERIAL

Figure S1. The effect of fenofibrate treatment on proteinuria, plasma albumin levels, and podocyte foot process effacement in DOX-treated BALB/c mice.
Figure S2. Measurement of BUN, serum creatinine and urinary KIM-1 levels in DOX-treated BALB/c mice.
Figure S3. Histological examination of the kidneys of DOX-treated BALB/c mice.
Figure S4. Immunohistochemistry, immunofluorescence and quantitative real-time PCR analysis of nephrin expression in the glomeruli of DOX-treated BALB/c mice.
Figure S5. The effect of fenofibrate treatment on proteinuria, plasma albumin levels, and podocyte foot process effacement in DOX-treated PPAR-α knockout mice.
Figure S6. Measurement of BUN, serum creatinine and urinary KIM-1 levels in DOX-treated PPAR-α knockout mice.
Figure S7. Renal histology examination in DOX-treated PPAR-α knockout mice.
Figure S8. Immunohistochemistry, immunofluorescence and quantitative real-time PCR analysis of nephrin expression in the glomeruli of DOX-treated PPAR-α knockout mice.
Figure S9. Effect of DOX treatment on expression of PPAR-α *in vivo* and *vitro*.
Figure S10. Ligand-induced transcriptional activity of PPAR-α in primary PPAR-α gene-deficient mesengial cells (PPAR-$\alpha^{-/-}$ MCs).
Figure S11. The protective effect of fenofibrate against DOX-induced apoptosis in renal glomeruli.
Figure S12. The influence of PPAR-α on DOX-induced ROS production in podocytes.
Figure S13. The time course of changes in proteinuria, plasma albumin levels, and podocyte foot process effacement in DOX-treated 129/SvJ mice.
Figure S14. The time course changes of BUN, serum creatinine and urinary KIM-1 levels in DOX-treated 129/SvJ mice.
Figure S15. Renal histology examination in DOX-treated 129/SvJ mice.
Figure S16. Immunohistochemistry, immunofluorescence and quantitative real-time PCR analysis of nephrin expression in the glomeruli of DOX-treated mice at different time points.
Figure S17. The condition of podocyte transfected with plasmids for PPRE-luciferase activity assay.

Supplementary material is linked to the online version of the paper at http://www.nature.com/ki

REFERENCES

1. Cheng H, Wang S, Jo YI *et al.* Overexpression of cyclooxygenase-2 predisposes to podocyte injury. *J Am Soc Nephrol* 2007; **18**: 551–559.
2. Koshikawa M, Mukoyama M, Mori K *et al.* Role of p38 mitogen-activated protein kinase activation in podocyte injury and proteinuria in experimental nephrotic syndrome. *J Am Soc Nephrol* 2005; **16**: 2690–2701.
3. Guo J, Ananthakrishnan R, Qu W *et al.* RAGE mediates podocyte injury in adriamycin-induced glomerulosclerosis. *J Am Soc Nephrol* 2008; **19**: 961–972.
4. Vogtlander NP, Tamboer WP, Bakker MA *et al.* Reactive oxygen species deglycosilate glomerular alpha-dystroglycan. *Kidney Int* 2006; **69**: 1526–1534.
5. Pippin JW, Brinkkoetter PT, Cormack-Aboud FC *et al.* Inducible rodent models of acquired podocyte diseases. *Am J Physiol Renal Physiol* 2009; **269**: F213–229.
6. Guan Y. Peroxisome proliferator-activated receptor family and its relationship to renal complications of the metabolic syndrome. *J Am Soc Nephrol* 2004; **15**: 2801–2815.
7. Auboeuf D, Rieusset J, Fajas L *et al.* Tissue distribution and quantification of the expression of mRNAs of peroxisome proliferator-activated receptors and liver X receptor-alpha in humans: no alteration in adipose tissue of obese and NIDDM patients. *Diabetes* 1997; **46**: 1319–1327.
8. Guan Y, Breyer MD. Peroxisome proliferator-activated receptors (PPARs): novel therapeutic targets in renal disease. *Kidney Int* 2001; **60**: 14–30.
9. Guan Y, Zhang Y, Davis L *et al.* Expression of peroxisome proliferator-activated receptors in urinary tract of rabbits and humans. *Am J Physiol* 1997; **273**: F1013–1022.
10. Portilla D. Energy metabolism and cytotoxicity. *Semin Nephrol* 2003; **23**: 432–438.
11. Duval C, Chinetti G, Trottein F *et al.* The role of PPARs in atherosclerosis. *Trends Mol Med* 2002; **8**: 422–430.
12. Park CW, Kim HW, Ko SH *et al.* Accelerated diabetic nephropathy in mice lacking the peroxisome proliferator-activated receptor alpha. *Diabetes* 2006; **55**: 885–893.
13. Park CW, Zhang Y, Zhang X *et al.* PPARalpha agonist fenofibrate improves diabetic nephropathy in db/db mice. *Kidney Int* 2006; **69**: 1511–1517.
14. Ruan X, Zheng F, Guan Y. PPARs and the kidney in metabolic syndrome. *Am J Physiol Renal Physiol* 2008; **294**: F1032–F1047.
15. Nagothu KK, Bhatt R, Kaushal GP *et al.* Fibrate prevents cisplatin-induced proximal tubule cell death. *Kidney Int* 2005; **68**: 2680–2693.
16. Lin H, Hou CC, Cheng CF *et al.* Peroxisomal proliferator-activated receptor-alpha protects renal tubular cells from doxorubicin-induced apoptosis. *Mol Pharmacol* 2007; **72**: 1238–1245.
17. Li S, Basnakian A, Bhatt R *et al.* PPAR-alpha ligand ameliorates acute renal failure by reducing cisplatin-induced increased expression of renal endonuclease G. *Am J Physiol Renal Physiol* 2004; **287**: F990–F998.
18. Li S, Wu P, Yarlagadda P *et al.* PPAR alpha ligand protects during cisplatin-induced acute renal failure by preventing inhibition of renal FAO and PDC activity. *Am J Physiol Renal Physiol* 2004; **286**: F572–F580.
19. Li S, Gokden N, Okusa MD *et al.* Anti-inflammatory effect of fibrate protects from cisplatin-induced ARF. *Am J Physiol Renal Physiol* 2005; **289**: F469–F480.
20. Kamijo Y, Hora K, Kono K *et al.* PPARalpha protects proximal tubular cells from acute fatty acid toxicity. *J Am Soc Nephrol* 2007; **18**: 3089–3100.
21. Fried LF, Orchard TJ, Kasiske BL. Effect of lipid reduction on the progression of renal disease: a meta-analysis. *Kidney Int* 2001; **59**: 260–269.
22. Kim H, Haluzik M, Asghar Z *et al.* Peroxisome proliferator-activated receptor-alpha agonist treatment in a transgenic model of type 2 diabetes reverses the lipotoxic state and improves glucose homeostasis. *Diabetes* 2003; **52**: 1770–1778.
23. Smulders YM, van Eeden AE, Stehouwer CD *et al.* Can reduction in hypertriglyceridaemia slow progression of microalbuminuria in patients with non-insulin-dependent diabetes mellitus? *Eur J Clin Invest* 1997; **27**: 997–1002##1997.
24. Negishi K, Noiri E, Maeda R *et al.* Renal L-type fatty acid-binding protein mediates the bezafibrate reduction of cisplatin-induced acute kidney injury. *Kidney Int* 2008; **73**: 1374–1384.
25. Ren S, Xin C, Beck KF *et al.* PPARalpha activation upregulates nephrin expression in human embryonic kidney epithelial cells and podocytes by a dual mechanism. *Biochem Biophys Res Commun* 2005; **338**: 1818–1824.
26. Vielhauer V, Berning E, Eis V *et al.* CCR1 blockade reduces interstitial inflammation and fibrosis in mice with glomerulosclerosis and nephrotic syndrome. *Kidney Int* 2004; **66**: 2264–2278.
27. Wang Y, Wang YP, Tay YC *et al.* Progressive adriamycin nephropathy in mice: sequence of histologic and immunohistochemical events. *Kidney Int* 2000; **58**: 1797–1804.
28. Okuda S, Oh Y, Tsuruda H *et al.* Adriamycin-induced nephropathy as a model of chronic progressive glomerular disease. *Kidney Int* 1986; **29**: 502–510.
29. Boonsanit D, Kanchanapangka S, Buranakarl C. L-carnitine ameliorates doxorubicin-induced nephrotic syndrome in rats. *Nephrology (Carlton)* 2006; **11**: 313–320.
30. Zhou Y, Zhang X, Chen L *et al.* Expression profiling of hepatic genes associated with lipid metabolism in nephrotic rats. *Am J Physiol Renal Physiol* 2008; **295**: F662–F671.
31. Ruan XZ, Varghese Z, Moorhead JF. An update on the lipid nephrotoxicity hypothesis. *Nat Rev Nephrol* 2009; **5**: 713–721.
32. Bobulescu IA. Renal lipid metabolism and lipotoxicity. *Curr Opin Nephrol Hypertens* 2010; **19**: 393–402.
33. van den Berg JG, van den Bergh Weerman MA, Assmann KJ *et al.* Podocyte foot process effacement is not correlated with the level of proteinuria in human glomerulopathies. *Kidney Int* 2004; **66**: 1901–1906.
34. Mundel P, Reiser J, Zuniga Mejia Borja A *et al.* Rearrangements of the cytoskeleton and cell contacts induce process formation during differentiation of conditionally immortalized mouse podocyte cell lines. *Exp Cell Res* 1997; **236**: 248–258.
35. Zheng F, Fornoni A, Elliot SJ *et al.* Upregulation of type I collagen by TGF-beta in mesangial cells is blocked by PPARgamma activation. *Am J Physiol Renal Physiol* 2002; **282**: F639–F648.